Heterogeneous fates and dynamic rearrangement of regenerative epidermis-derived cells during zebrafish fin regeneration

Eri Shibata[1], Kazunori Ando[1], Emiko Murase[1], and Atsushi Kawakami[1,*]

[1] School of Life Science and Technology, Tokyo Institute of Technology, 4259 Nagatsuta, Midori-ku, Yokohama 226-8501, Japan.

*Author for correspondence (e-mail: atkawaka@bio.titech.ac.jp)

KEY WORDS: Zebrafish, Fin regeneration, Wound epidermis, Cell lineage, Fibronectin 1b, Cre-loxP

Summary: Fate of regenerative epidermis during zebrafish fin regeneration has been elucidated. Cell of regenerative epidermis transiently contribute to the regenerated epidermis, but many are expelled by dynamic epidermal rearrangement.

ABSTRACT

The regenerative epidermis (RE) is a specialized tissue that plays an essential role in tissue regeneration. However, the fate of the RE during and after regeneration is unknown. In this study, we performed Cre-*loxP*-mediated cell fate tracking and revealed the fates of major population of regenerative epidermis cells that express *fibronectin 1b* (*fn1b*) during zebrafish fin regeneration. Our study showed that these RE cells are mainly recruited from the inter-ray epidermis, and that they follow heterogeneous cell fates. Early recruited cells contribute to initial wound healing and soon disappear by apoptosis, while the later recruited cells contribute to the regenerated epidermis. Intriguingly, many of these cells were also expelled from the regenerated tissue by a dynamic caudal movement of the epidermis over time, and in turn the loss of epidermal cells was replenished by a global self-replication of basal and suprabasal cells in fin. De-differentiation of non-basal epidermal cells into the basal epidermal cells did not occur during regeneration. Overall, our study revealed heterogeneous fates of RE cells and a dynamic rearrangement of the epidermis during and after regeneration.

INTRODUCTION

One of the important roles of the epidermis is to protect the internal homeostasis of multicellular organisms from the external stresses, including mechanical and chemical damage, pathogens, and radiation (Chuong, et al., 2002). In mammals, the epidermis is composed of several distinct cell layers. The horny layer at the surface contains layers of keratinized cells. The granular layer provides a hydrophobic barrier underneath the horny layer. The spinous layer is a thick layer that contains a number of differentiating keratinocytes. In the deepest part of the skin, a layer of basal stem cells constantly produces new keratinocytes to maintain epidermal tissue homeostasis (reviewed by Fuchs, 2008).

Teleost fish, including zebrafish, have a similar layered structure in their epidermis, although the outermost layer is not covered by a horny layer, but rather by a mucous layer (Rakers et al., 2013). Apart from structural similarity, the process of cell turnover in zebrafish is nearly the same as that observed in mammals, in that the basal stem cells produce all the strata of the epidermis (Lee et al., 2014). Thus, the zebrafish epidermis is thought to be a useful model to investigate the regulatory mechanisms involved in skin homeostasis and regeneration. In particular, zebrafish fins, which are devoid of dermal tissues including the typical connective tissues and muscles, have an advantage for fluorescent live-imaging using a standard confocal microscope.

Additionally, unlike mammals, which do not completely regenerate tissues after massive injury, but instead form scars, teleost fish can perfectly reform their lost appendages through a process called epimorphic regeneration. In addition, the layered epidermal structure is also completely reformed without the formation of scars. An analysis of this scar-less skin regeneration process in zebrafish could lead to the development of regenerative medicine aimed at perfect skin regeneration.

In the process of epimorphic regeneration, epithelial cells migrate to cover the wound after amputation and form a thick epithelium, which is referred to as the wound epidermis (WE). However, the term of WE has been used without clear definition. Numerous studies have shown that regeneration is impaired by disturbing the normal formation of the WE and by surgically removing the WE (Goss, 1956; Thornton, 1957; Mescher, 1976; Tassava and Garling, 1979), suggesting that the WE is an epidermal tissue that is required for inducing blastema formation, and is essential for regeneration (reviewed by Campbell and Crews, 2008). Recent studies in zebrafish have suggested that the WE directs blastema formation through fibroblast growth factor signalling (Shibata et al., 2016), and that the alignment of osteoblast progenitors during fin regeneration is regulated by the Sonic hedgehog signalling in the WE (Armstrong et al., 2017). However, the definition of the WE is controversial, because the term WE was sometimes used as the epithelial layers formed within a few hours following injury. In this paper, we refer the epidermal cells covering the regenerate during regeneration as the “regenerative epidermis (RE)”.

Thus, an increasing body of data suggests that the RE plays an important role in tissue regeneration. However, no studies have investigated the origin and fate of RE cells, and whether corresponding cells are found during mammalian skin regeneration. Elucidation of the origin and fate of the RE cells during/after regeneration is an important goal in understanding the mechanism of perfect epidermal regeneration. Recently, Chen et al. (2016) have generated *Skinbow* transgenic zebrafish, in which they tracked superficial epidermal cells and demonstrated the dynamic behaviour of superficial epidermal cells. However, thus far, no studies have addressed the origin and fate of the RE cells, and how the cells required for the formation of the regenerated epidermis are supplied during regeneration.

Here, we reveal the origin and the fate of RE cells using *fibronectin 1b* (*fn1b*) as a regenerative epidermis marker and genetic cell fate tracking. We found that RE cells are mainly recruited from epidermal cells of the inter-ray regions, and that they contribute to the regenerated epidermis with the exception of the early recruited cells that are immediately lost by apoptosis following wound healing. Unexpectedly, after contributing the regenerated epidermis, many of the epidermal cells derived from the RE are lost from the fin by a dynamic caudal movement of the epidermis, and the epidermal cells are replenished by a global activation of cell proliferation. We further show that de-differentiation of non-basal epidermal cells into the basal epidermal cells does not occur during regeneration. Our study has revealed heterogeneous fates of the RE cells and a dynamic rearrangement of the epidermis during and after regeneration.

RESULTS

The inter-ray epidermis mainly contribute to the RE

Our previous study has shown that *fn1b* is highly upregulated in the RE during zebrafish fin regeneration (Yoshinari et al., 2009). A detailed expression analysis of *fn1b* in the adult zebrafish fin showed that mRNA expression was first detected at 0.5 day post amputation (dpa) in the epithelial cells near the amputation plane and then expanded to the entire region of the newly formed RE at 1 dpa (Fig. 1A). At 2 dpa and thereafter, *fn1b* mRNA expression became weaker in the outermost layer and distal region, and was confined to the basal and suprabasal cells of the inter-ray RE and the suprabasal cells of the ray RE (Fig. 1A; Fig. S1). Thus, the expression of *fn1b* is consistently observed in the epidermis covering the blastema, indicating that *fn1b* is a useful RE marker that is expressed in many RE cells.

To assess the behaviour of RE cells, we generated a BAC transgenic (*Tg*) line, *Tg(fn1b:egfp)*, that recapitulates *fn1b* expression (Fig. 1B; Fig. S2). In the *Tg*, EGFP expression was low in the uncut fin (Fig. 1C), but following amputation, strong EGFP expression, which resembled that detected by *in situ* hybridization (ISH) analysis of *fn1b* expression, was observed from 1 dpa and thereafter (Fig. 1D). Though the timing of EGFP expression is slightly delayed, this is reflective of the time required for

the EGFP protein to mature. The intensity of EGFP expression gradually decreased after 4 dpa, although fluorescence was still slightly detectable at 6 dpa (Fig. 1E). EGFP expression in the RE was further confirmed by immunohistochemical staining of the section of the *Tg* fin with an antibody against E-cadherin, an epithelial cell marker (Fig. 1F).

EGFP expression was high in the inter-ray regions at 1 dpa, and further confined to the inter-ray regions at 2 dpa (Fig. 1D). Moreover, the regenerating tissue showed a striped wavy pattern of EGFP$^+$ cells (Fig.1G), suggesting a possibility that many of the EGFP$^+$ cells were derived from the inter-ray regions and had migrated distally and laterally to cover the whole amputation plane. To further confirm this, we performed time-lapse observation of EGFP$^+$ cells over 300 min from 24 hours post amputation (hpa). The analysis supported the notion that EGFP$^+$ cells indeed migrated from the inter-ray epidermis and spread over the ray region (Fig.1H, white arrowheads). Considering the *fn1b* expression in the ray epidermis at 0.5 dpa, a stage before the migration of *fn1b*$^+$ inter-ray cells (Fig. 1A), it is thought that the epidermal cells from ray and inter-ray regions together form the RE in the ray region.

Fate tracking of *fn1b*$^+$ RE cells

Thus, the observation made in the *Tg(fn1b:egfp)* suggested that *fn1b*$^+$ RE cells are mainly recruited from the inter-ray epidermis. However, it is still possible that cells dynamically change *fn1b* expression during tissue regeneration. To determine the actual cell fate of *fn1b*$^+$ cells, we developed an additional *Tg* line that expresses CreERt2 under the regulation of the *fn1b* promoter (Fig. 2A). CreERt2 is a version of Cre bacterial recombinase that has a high affinity for the oestrogen analogue, 4-OH tamoxifen (TAM). When double *Tg(fn1b:creERt2;Olactb:loxP-dsRed2-loxP-egfp)* (Yoshinari et al., 2012) were treated with TAM to induce Cre-*loxP* recombination following fin amputation, we successfully observed the appearance of EGFP$^+$ cells (Fig. 2B), while EGFP$^+$ cells were rarely seen in uncut fins (data not shown) or amputated fins without TAM treatment (Fig. 2C). More importantly, EGFP$^+$ cells were observed in both the basal and superficial epidermal cells, suggesting that there is no biased Cre-*loxP* labelling of *fn1b*$^+$ cells to specific epidermal cell types (Fig. 2D).

By using these double *Tg*, we labelled the *fn1b*$^+$ RE cells by treatment with TAM at 0–24 hpa and tracked their cell fate between 24–48 hpa (Fig. 2E). As in the *Tg(fn1b:egfp)*, Cre-labelled cells were first detected in the inter-ray epidermis and also migrated to cover the fin rays and form the RE (Fig. 2E). Although a previous study has suggested that RE cells are recruited from the proximal epidermal cells (Nakatani et al., 2008), our analysis further showed that many epidermal cells that migrate from the inter-ray region contribute to RE formation.

To further investigate the initial process of RE formation earlier than 24 hpa, we re-amputated the regenerating fins in which the RE cells were labelled by Cre recombination. As we describe in the later section (Fig. 4), a group of Cre-labelled RE cells contribute to the regenerated epidermal cells. Consistent with the above observation during 24–48 hpa, the epidermal cells in the inter-ray region contributed to both the ray (44%) and inter-ray RE (56%), while those in the ray region only contributed to the ray RE (Fig. S3). These observations support that the epidermal cells from ray and inter-ray regions together form the ray RE.

Early RE cells are discarded within 5 dpa by apoptosis

To dissect the processes of RE formation and the fate of its component cells, we performed pulse labelling of *fn1b*$^{+}$ cells and tracked their fate. First, labelling was performed with 0.1 μM TAM over the wound healing and early RE formation stage at 9–10 hpa (Nechiporuk and Keating, 2002). Cre-labelled cells began to be detected at 1 dpa, and were clearly observed at 2 dpa in distally localised superficial regions of the RE (Fig. 3A).

When these cells were tracked at subsequent stages, they were further confined to the distal fin edge and disappeared by 5 dpa (Fig. 3A, B). Many of the Cre-labelled cells were positive for TdT-mediated dUTP nick end labelling (TUNEL) staining of apoptotic cells, indicating that these cells are discarded through apoptosis (Fig. 3C). Thus, these data suggest that the early *fn1b*-expressing cells found during wound healing and early RE formation stages are mainly recruited from the inter-ray epidermis to transiently cover the wound, but they are unable to form the regenerated epidermis, and soon vanish from the regenerating epidermis by undergoing apoptosis.

Later RE cells contribute to the regenerated epidermis

We next tracked later-arising RE cells by inducing Cre recombination during 24–25 hpa, a stage when RE formation is already evident. After labelling, Cre-labelled cells were detected by 2 dpa, mainly in the inter-ray epidermis, and in contrast to the early labelling at 9–10 hpa, EGFP^{+} cells and their progeny were observed in both the basal and superficial layers of the RE, and survived beyond 5 dpa, although the number of cells decreased as the stage proceeded (Fig. 4A). In subsequent stages, these surviving EGFP^{+} cells proliferated to form colonies within the regenerated epidermis at 14 dpa.

When Cre recombination was induced at a further later stage of fin regeneration (i.e. during 2–5 dpa), the overall fate of the RE cells was similar to that seen in Fig. 4A. The later RE cells and their progeny formed a number of colonies by 1 week post amputation (wpa); however, 80% of colonies had disappeared by 3 wpa (Fig. 4B, C). In contrast to the decrease in the number of colonies, the size of the colonies increased approximately 6.5 times between 1–3 wpa (Fig. 4D). After 3 wpa, the number of colonies further declined; however, some progeny remained in the fin

epidermis maintaining their size for more than 4 months (Fig. 4E). Taken together, the fate tracking analysis of later-arising RE cells revealed that a population of progeny of the RE cells actually contribute to the regenerated epidermis though many of the RE-derived colonies disappear from the regenerated epidermis by 3 wpa.

Fate tracking of RE-derived epidermal clones

The fate tracking studies described above showed that many of the RE progeny are lost from the regenerated tissue, with the exception of a fraction of them. We next questioned how these different fates arise. To do this, we conducted single cell fate tracking of RE cells by inducing sparse Cre-labelling. It has been reported that the fulvestrant (ICI), an antagonist for the oestrogen receptor, induces the CreERt2 recombination in cultured cells (Metzger et al., 1995; Feil et al., 1997). By applying 2.5 μM ICI during the period 2–3 dpa, we successfully labelled a small number of RE cells (Fig. 5A). Well-isolated $EGFP^+$ colonies, each of which is considered to be a clone derived from a single RE cell, were randomly selected from both the proximal and distal regions at 5 dpa, and their fates were tracked every day by comparing their positions and morphologies. Furthermore, cell types and numbers composing the respective clones were determined every other day by analysing z-stack confocal images (Fig. S4; Table S1).

The results of single clone tracking experiment were similar to those in Fig. 4B. Many of $EGFP^+$ clones (27 out of 41, 65.9%) disappeared by 15 dpa (Fig. 5B). At 5 dpa, one of them (2.4%) contained only surface cells, whereas the rest were composed of either basal (68.3%) or suprabasal (29.3%) cells. As regeneration proceeds, the clones containing only the suprabasal cells became the clones containing both suprabasal and surface cells by 7 dpa, and finally became the clones containing only the surface cells at 15 dpa (Fig. 5C). Many of the basal cell clones at 5 dpa also produced suprabasal and surface cells during regeneration, but they retained basal cells at 15 dpa, resulting in clones containing all three epidermal cell types (Fig. 5C). These observations suggest that epidermal cellular turnover begins right after formation of the regenerated epidermis as it does in normal epidermis and that the presence of basal cells is essential for maintaining long-lasting epidermal clones.

With respect to cell proliferation, some clones without basal cells (circles painted in blue, Fig. 5B) showed increases in cell numbers during regeneration (Nos. 6, 10, 23, and 24 in Fig. 5B), but they stopped to proliferate or disappeared by 15 dpa. Although almost all of the clones that were retained at 15 dpa (marked with the thick blue outline) were basal cell-containing clones (circles painted in red, Fig. 5B), different proliferation patterns were observed between them; for example there were clones with almost no proliferation (Nos. 18, 32, and 40), clones with continuous proliferation (Nos. 12, 25, 26, 34, 36, 38, 39, and 41), and clones that initially proliferated, but later decreased their size (Nos. 27, 33, and 35). Significantly, it appeared that these clones with different

proliferative profiles were distributed at random, suggesting that the RE-derived epidermal clones stochastically adopt heterogeneous proliferative fates.

RE cells in the distal region are discarded after regeneration

Importantly, fate tracking of RE-derived epidermal clones showed that many of the clones, even clones with basal cells and/or an active cell proliferation profile, also disappeared by 15 dpa (Fig. 5B). By plotting the initial position within the fins of respective clones that were survived or disappeared at 15 dpa, we found that clones surviving beyond 15 dpa (circles with a blue edge, Fig. 5B) were mostly situated within proximal half of the regenerates in 5 dpa fins (Fig. 5D), and that clones in the distal region were moved caudally and expelled from the regenerated fin, revealing that much of the epidermal cells derived from the later RE transiently contributes to the regenerated epidermis and are lost from fin as a result of dynamic epidermal movement to the distal direction. It is thought that cells reaching to fin edge disappear either by apoptosis or by simple detachment from fin edge; however, we were unable to verify these possibilities due to the always occurring apoptosis at the fin edge.

De-differentiation of epithelial cells does not occur during regeneration

In homeostatic epidermal cell turnover, suprabasal cells, committed progenitor cells, or differentiated keratinocytes do not produce basal stem cells in mammalian skin. However, studies have reported that during epimorphic regeneration of amphibian limbs and fish fins, de-differentiation of mature muscle cells or osteoblasts to form proliferative progenitor states can occur (Sandoval-Guzmán et al., 2014; Knopf et al., 2011; Geurtzen et al., 2014). Thus, it is possible that de-differentiation of suprabasal cells or surface epidermal cells, and the resulting supply of basal cells could enable perfect skin regeneration.

To examine this possibility, we generated an additional transgenic line that express CreERt2 under control of the *keratin4* (*ker4*) promoter, which is known to be activated in the non-basal layer epidermis (Wehner et al., 2013; Fig. S5) and tracked the fate of suprabasal and/or surface cells in the epidermis. At 2 days after treatment of the double *Tg(krt4:creERt2;Olactb:loxP-dsRed2-loxP-egfp)* with TAM for 24 h (Fig. 6A), $EGFP^+$ cells appeared in the epidermis of uncut fins (Fig 6B), mainly in the suprabasal and surface cell layers (Fig. 6C), indicating that the suprabasal and surface cells had been successfully labelled. In contrast, TAM-independent Cre-recombination was rarely observed in uncut fins or amputated fins without TAM treatment (Figs. 6D).

At 2 days after TAM treatment, fin amputation was performed, and the fates of $EGFP^+$ cells were analysed by identifying the epidermal cell types from the z-stack images of confocal microscopy. The results revealed that most of the $EGFP^+$ cells were observed in the non-basal layers like the suprabasal and the surface layers (Fig. 6E). Since a small proportion of the $EGFP^+$ cells (2.7%) were detected among basal cells in uncut fins following TAM treatment (Fig. 6F), the numbers of $EGFP^+$

cells in the basal and non-basal layers were quantified and compared to those before and after fin amputation. The fraction of basal cells within the $EGFP^+$ cells was 1.7% at 3 dpa, which was unchanged from that before amputation, indicating that suprabasal and surface cells of the epidermis do not extensively de-differentiate into basal cells during fin regeneration.

Global activation of cell proliferation replenishes the epidermal cells

The finding that the many of the regenerated epidermal clones are lost within a few weeks of regeneration raised a further question how the lost epidermal cells are replenished. It is thought that new epidermal cells are supplied by an increase in basal cells, either locally in the adjacent proximal region or globally in the entire fin.

To explore these possibilities, we performed EdU labelling of proliferating cells at 10 dpa fins, a stage when the RE-derived epidermal cells are rapidly lost (Fig. 5B), and compared the number of EdU^+ cells in different fin regions to those in uncut fins (Fig. 7A). In uncut side of fins, only a few EdU^+ nuclei were uniformly detected in different fin regions (Fig. 7B), although non-basal cells have a higher proliferative index than basal cells (Fig. 7C). In amputated side of fins, an apparent increase in the number of EdU^+ nuclei was observed both in basal and non-basal cells of the epidermis (Fig. 7D–F). Importantly, EdU^+ nuclei were equally distributed both in the distal region, which is adjacent to the area from where the RE-derived epidermal cells are lost, and the proximal fin regions distant from the RE-derived epidermis (Fig. 7D–G), indicating that new epidermal cells are replenished by a global activation of epidermal cell proliferation.

More importantly, when the 3D-distribution of EdU^+ cells was analysed from the captured confocal z-stack images, an increase in EdU^+ cells in the amputated side was detected among both the basal cells and non-basal cells of the epidermis (Fig. 7G). Therefore, these data suggest that both basal and non-basal cell proliferation replenish the lost epidermal cells in the distal fin area during and after regeneration, and that the increased proliferation of the basal cells in the entire fin region is crucial for providing long-lasting epidermal clones.

DISCUSSION

It has been suggested that the epidermis at the wounded site plays an essential role in regeneration (Goss, 1956; Thornton, 1957; Mescher, 1976; Tassava and Garling, 1979). However, the fate of the RE during and after regeneration has remained unclear. In this study, we performed Cre-*loxP*-mediated cell fate tracking, using *fn1b* as a marker induced in the RE, and succeeded in revealing the fates of the RE cells. Our study revealed heterogeneous cell fates of epidermal cells derived from the major RE cells expressing *fn1b* and further demonstrated the existence of a dynamic and global rearrangement of the epidermis during and after regeneration.

In this study, we successfully used *fn1b* as a maker of the RE to label many of the RE cells. In amphibian limb regeneration, the RE has been defined by its thick and layered morphology and the expression of characteristic genes such as MMPs, FGFs and collagens (Campbell and Crews, 2008). In zebrafish fin regeneration, previous studies have shown that genes such as *igfr1* (Chablais and Jaźwińska, 2010), *laminin beta 1a* (Chen et al., 2015), *fgf20a* (Shibata et al., 2016), and *sonic hedgehog* (Armstrong et al., 2017) are expressed in the RE; however, the expression of these genes is restricted to the basal layer of the RE. Since *fn1b* is expressed in all strata of the RE (Fig. 1A, D), *fn1b* is a better marker to label all types of the RE cells. As we have previously reported that *junb* is also expressed in the RE from an early stage of regeneration (Yoshinari et al., 2008), *junb* could also be an alternative gene that could be used for labelling RE cells.

Our live-imaging experiment using the *fn1b Tg* revealed that RE cells are recruited mainly from the inter-ray region. A previous study by Poleo et al. (2001) used DiI to trace the short-term fate of the RE and suggested that epidermal cells far proximal to the amputation site migrate to form the RE. Recently, Chen et al. (2016) have traced the fates of the superficial epidermal cells using *Skinbow* zebrafish and reported that superficial epidermal cells in the inter-ray region have a higher cellular mobility than those of ray superficial cells during wound healing. This observation is consistent with ours, in that many of the RE cells originate from the superficial inter-ray epidermis.

Using cell fate tracking, we also demonstrated that RE cells recruited early in the wound healing process disappear through apoptosis by 5 dpa. The occurrence of such early RE cell apoptosis is consistent with an observation reported by Gauron et al. (2013), in which they detected apoptotic cells among epidermal cells during regeneration and wound healing. Because the early (i.e. before 12 hpa) migrating epidermal cells display little or no cell proliferation (Nechiporuk and Keating, 2002; Jaźwińska et al., 2007), it is thought that the epidermal cells around the wound are recruited to the wounded site without cell proliferation in order to efficiently make a transient epidermal seal over the wound. It is possible that these short-lived cells could also play an additional role in regeneration, because Gauron et al. (2013) have reported that inhibition of apoptosis in epidermal cells impaired blastema formation.

Our study has revealed for the first time that the lately-recruited RE cells actually contributes to the regenerated epidermis. However, unexpectedly, we also found that the RE-derived cells in the distal region are expelled by movement of the epidermal sheet in the caudal direction, and in turn, following loss of these epidermal cells, they are replenished by a global activation of cell proliferation in nearly the entire area of the fin. These results raise further questions as to why the distal RE-derived epidermal cells are discarded, and how a cell proliferation signal reaches proximal fin regions far away from the wound; these questions will be the subjects of future studies.

Furthermore, it is also intriguing to note that the proliferation of the respective RE-derived epidermal clones occurs at random, independent of their positions (Fig. 5B). It has also been recently suggested that the basal layer contains heterogeneous stem cell populations in mice, which show different patterns of proliferation and differentiation during homeostasis and regeneration (Sada, et al., 2016). It is possible that the basal cells are heterogeneous in advance and that their proliferative abilities could be related to their aging status and/or numbers of cell division they have undergone. Alternatively, it is also conceivable that proliferative and differentiation capacity is stochastically determined within homogeneous progenitor cells (Clayton et al. 2007).

More significantly, cell tracking of non-basal cells suggested that de-differentiation of non-basal cells into basal cells does not occur during regeneration (Fig. 6). In some cases, such as regeneration of muscle during newt limb regeneration (Sandoval-Guzmán et al., 2014) or of osteoblasts during zebrafish fin regeneration (Knopf et al., 2011; Geurtzen et al., 2014), proliferating cells are generated by cell de-differentiation during regeneration. However, we did not detect an apparent and extensive de-differentiation of the non-basal epidermal cells into basal stem cells during fin regeneration, suggesting the importance of self-renewal of basal stem cells for epidermal regeneration. However, the process of perfect skin reformation during the epimorphic regeneration was not strikingly different from that of mammalian skin repair and renewal. It is thought that this is also true for the trunk and other skin regions of zebrafish, and therefore the difference of regenerative abilities between fish and mammalian skin is possibly due to the proliferative ability of the basal stem cells. Elucidation of the control mechanism for self-renewal of basal stem cells should therefore open a way to developing scar-less regeneration or rejuvenation in mammalian skin.

MATERIALS AND METHODS

Zebrafish strains and genetics

WT zebrafish (*Danio rerio*) strain, which was originally derived from the Tubingen strain and has been maintained in our facility for more than 10 years by inbreeding, and all transgenic lines were kept in a recirculating water system with a 14-hr day/10-hr night photoperiod at 28.5°C. *Tg(krt4p:gal4)* (Wada et al., 2013) and *Tg(UAS:GFP)* (Asakawa et al., 2008) were generous gifts from Hironori Wada and Koichi Kawakami, respectively. All animal procedures were approved by the Animal Care and Use Committee at the Tokyo Institute of Technology. All the animals were handled according to the Animal Research Guidelines of the Tokyo Institute of Technology. All surgical procedures were performed under tricaine (3-aminobenzoic acid ethyl ester) anaesthesia, and every effort was made to minimize suffering. Experiments on adult regeneration were performed using 3- to 12-month-old adult zebrafish.

Fin amputation

Fin amputation was performed under anaesthesia with 0.002 % tricaine (3-aminobenzoic acid ethyl ester, Sigma-Aldrich) and the caudal fins were cut in a straight line using a scalpel. For the single cell tracking experiment shown in Fig. 5, fins were amputated at a position 1 mm distal from the root of the fin. For other experiments, fins were amputated at the middle position of the central fin ray.

Transgenic zebrafish

BAC recombineering and generation of *fn1b Tgs* were performed as described previously (Ando et al., 2017). The *egfp* or *creERt2* cassettes for BAC recombineering were amplified by PCR using the following primers. Fn1b egfp fw, 5'-agccgaaatacagtcaaagccagaagctgctctccataacgcgggtgaaaATGGTGAGCAAGGGCGAGGA-3'; fn1b egfp rv, 5'- ggcttgtcttttacttttccctgcggattgtggcatgcagtggacagTCAGAAGAACTCGTCAAGAAGGC-3'. Fn1b creERt2 fw, 5'-cgaaatacagtcaaagccagaagctgctctccataacgcgggtgaaaATGTCCAATTTACTGACCGTACA-3'; fn1b creERt2 rv, 5'-ggcttgtcttttacttttccctgcggattgtggcatgcagtggacagatcCACAGGATCAAGAGCACCCG-3'

By crossing the founder F0 zebrafish with each other, or with WT zebrafish, zebrafish lines expressing EGFP were obtained. As all of these lines displayed indistinguishable levels of EGFP expression, one line was selected to establish the *Tg(fn1b:egfp)*. The *Tg(fn1b:creERt2)* was first screened for EGFP expression in the lens and then tested for Cre recombination by treating with TAM in the adult amputated fin. One F0 line that had a distribution of Cre-labelled cells consistent with that of *Tg(fn1b:egfp)* was identified, and was established as the Cre-expressing line.

Tg(krt4:mchrerry-t2a-creERt2) was generated by replacing the heat shock promoter of *pTol2(hsp70l:mcherry-t2a- creERt2)* (Yoshinari et al., 2012) with the *krt4* promoter using the SfiI sites. The plasmid DNAs at a concentration 25 ng/μL were injected, along with 25 ng/μL transposase mRNA, into fertilized eggs at the one-cell-stage.

Whole-Mount ISH

Whole-mount ISH was performed according to a standard protocol (Thisse and Thisse, 2008). For RNA probe generation, a region of the *fn1b* coding sequence was amplified by PCR using the following primers.

fn1b fw, 5′-GCATGTGTCATGGACCGCAC-3′; *fn1b* rv: 5′-AGCGTACAGTCAAGGTATTG-3′

The PCR product was cloned into pCR4 vector (Clontech). The *egfp* probe was synthesized from pCS2-*egfp*, which harbours the *egfp* sequence in the pCS2 vector.

Immunostaining and Histological Methods

Immunostaining was performed as described previously (Shibata et al., 2016). Anti-E-cadherin antibody (BD Transduction Laboratories) was used at 500 ng/mL. The anti-GFP antibody (Nacalai Tesque) was used at a 1:1000 dilution. Fins were mounted in 80% glycerol containing 25 mg/mL triethylenediamine (DABCO, Nacalai Tesque) as an anti-fading reagent. Images were obtained using a confocal microscope. Cell death was detected by TUNEL staining, as described previously (Hasegawa et al., 2017).

Cre-*loxP* Recombination and Lineage Tracking

The *Tg* strains carrying *fn1b:creERt2* or *krt4:creERt2* were crossed with the *Tg(Olactb:loxp-dsred2-loxp-egfp)* (Yoshinari et al., 2012) strain to generate the double *Tg* zebrafish. Cre-*loxP* recombination was induced by treating the *Tgs* with either 4-OH TAM (Sigma-Aldrich) or ICI (Sigma-Aldrich) in fish water (0.3% artificial sea salt, 0.0001% methylene blue). The conditions for Cre-*loxP* recombination are indicated in the respective figure legends.

Quantification of Cre-labelled cells

The number and area of the epidermal cell colonies that were derived from the Cre-labelled RE cells (Fig. 4C, D) were quantified using ImageJ software (ver1.49; https://imagej.nih.gov/ij/). To measure colony area, fluorescent images were obtained using a stereoscopic microscope and were binarized by applying a colour threshold (Red-Green-Blue colour model) to select only the areas appearing in green and analysed using the 'analyse particles' command in ImageJ software.

Time-Lapse Recording of Cre-labelled cells

For live imaging of the *Tgs*, zebrafish were anaesthetized with 0.002% tricaine. Fins were embedded in 1.5% low melting point agarose gel and observed under a 40 × water-immersion objective lens using a confocal laser scanning microscope (LSM780, Carl Zeiss). For single cell tracking, confocal images were captured at intervals of two days.

Detection of Cell Proliferation and Quantification

Proliferating cells were detected by EdU labelling using the Click-iT EdU Imaging Kit (Thermo Fisher Scientific), as described previously (Shibata et al., 2016). Only the dorsal half of the fins was amputated at the mid position of the central fin ray, while the ventral half of the fin was used as an uncut control. Zebrafish were incubated in a solution containing 50 μM EdU in fish water for 6 hours at 28.5°C before fin fixation. After EdU detection, samples were counter-stained with DAPI (0.1 μg/mL in PBS containing 0.1% Triton X-100 (PBTx), washed with PBTx, and mounted in 80% glycerol containing DABCO. The third fin rays from the dorsal (regenerated) or ventral sides (uncut)

were used for scoring EdU^+ cells. The epidermal or non-epidermal identities of EdU^+ cells were determined on the captured confocal z-stack images by using the ZEN microscope software (Carl Zeiss).

Statistics

Clutch-mates were randomized into different treatment groups for each experiment. All experiments were performed with at least two biological replicates, using the appropriate number of samples for each replicate. Sample sizes are indicated in each figure legend. For expression patterns, at least five zebrafish were examined. Statistical analyses were performed using Microsoft Excel 2013. All statistical values are displayed as mean ± standard error of the mean. Sample sizes, statistical tests, and *p* values are indicated in the respective figure legends. Student's *t*-tests (two-tailed) were applied when normality and equal variance tests were passed (Figs. 5D, 6F and 7G).

Acknowledgments

We thank Hiroshi Wada (Kitasato University) for providing the *Tg(krt4p:gal4)* line, and Koichi Kawakami (National Institute of Genetics, Mishima) for the *Tg(UAS:GFP)* line. This work was supported by grants from the Koyanagi Foundation, Grant-in-Aid for Scientific Research (C) (16K07365) and Grants-in-aid for Scientific Research on Innovative Areas "Stem Cell Aging and Disease" (17H05637) to A. K. E.S. and K.A. were supported by fellowships from the Education Academy of Computational Life Science (ACLS) of the Tokyo Institute of Technology.

Competing interests

The authors declare that they have no competing financial interests.

Author contributions

E. S., K. A., E. M. and A. K. designed the experimental strategy, conducted experiments and analysed the data; and E. S. and A. K. prepared the manuscript. All authors approved the manuscript.

Funding

This work was supported by grants from the Koyanagi Foundation, a Grant-in-Aid for Scientific Research (C) (16K07365) and Grants-in-aid for Scientific Research on Innovative Areas "Stem Cell Aging and Disease" (17H05637) to A. K.

Supplementary information

Supplementary information is available online at

http://dev.biologists.org/lookup/suppl/xxxxxxx

References

Ando, K., Shibata, E., Hans, S., Brand, M. and Kawakami, A. (2017). Osteoblast Production by Reserved Progenitor Cells in Zebrafish Bone Regeneration and Maintenance. *Dev. Cell* **43**, 643–650.

Armstrong, B. E., Henner, A., Stewart, S. and Stankunas, K. (2017). Shh promotes direct interactions between epidermal cells and osteoblast progenitors to shape regenerated zebrafish bone. *Development* **144**, 1165–1176.

Asakawa, K., Suster, M. L., Mizusawa, K., Nagayoshi, S., Kotani, T., Urasaki, A., Kishimoto, Y., Hibi, M. and Kawakami, K. (2008). Genetic dissection of neural circuits by Tol2 transposon-mediated Gal4 gene and enhancer trapping in zebrafish. *Proc. Natl. Acad. Sci. U.S.A.* **105**, 1255–1260.

Campbell, L. J. and Crews, C. M. (2008). Wound epidermis formation and function in urodele amphibian limb regeneration. *Cell. Mol. Life Sci.* **65**, 73–79.

Chablais, F. and Jaźwińska, A. (2010). IGF signaling between blastema and wound epidermis is required for fin regeneration. *Development* **137**, 871–879.

Chen, C.-H., Merriman, A. F., Savage, J., Willer, J., Wahlig, T., Katsanis, N., Yin, V. P. and Poss, K. D. (2015). Transient laminin beta 1a induction defines the wound epidermis during zebrafish fin regeneration. *PLOS Genet.* **11**, e1005437.

Chen, C.-H., Puliafito, A., Cox, B. D., Primo, L., Fang, Y., Di Talia, S. and Poss, K. D. (2016). Multicolor cell barcoding technology for long-term surveillance of epithelial regeneration in zebrafish. *Dev. Cell* **36**, 668–680.

Chuong, C. M., Nickoloff, B. J., Elias, P. M., Goldsmith, L. A., Macher, E., Maderson, P. A., Sundberg, J. P., Tagami, H., Plonka, P. M., Thestrup-Pederson, K., et al. (2002). What is the "true" function of skin? *Exp. Dermatol.* **11**, 159–187.

Clayton, E., Doupé, D. P., Klein, A. M., Winton, D. J., Simons, B. D. and Jones, P. H. (2007). A single type of progenitor cell maintains normal epidermis. *Nature* **446**, 185–189.

Feil, R., Wagner, J., Metzger, D. and Chambon, P. (1997). Regulation of Cre recombinase activity by mutated estrogen receptor ligand-binding domains. *Biochem. Biophys. Res. Commun.* **237**, 752–757.

Fuchs, E. (2008). Skin stem cells: Rising to the surface. *J. Cell Biol.* **180**, 273–284.

Gauron, C., Rampon, C., Bouzaffour, M., Ipendey, E., Teillon, J., Volovitch, M. and Vriz, S. (2013). Sustained production of ROS triggers compensatory proliferation and is required for regeneration to proceed. *Sci. Rep.* **3**, 2084.

Geurtzen, K., Knopf, F., Wehner, D., Huitema, L. F. A., Schulte-Merker, S. and Weidinger, G. (2014). Mature osteoblasts dedifferentiate in response to traumatic bone injury in the zebrafish fin and skull. *Development* **141**, 2225–2234.

Goss, R. J. (1956). Regenerative inhibition following limb amputation and immediate insertion into the body cavity. *Anat. Rec.* **126**, 15–27.

Hasegawa, T., Hall, C. J., Crosier, P. S., Abe, G., Kawakami, K., Kudo, A. and Kawakami, A. (2017). Transient inflammatory response mediated by interleukin-1β is required for proper regeneration in zebrafish fin fold. *Elife* **6**, 1–22.

Jaźwińska, A., Badakov, R. and Keating, M. T. (2007). Activin-βA signaling is required for zebrafish fin regeneration. *Curr. Biol.* **17**, 1390–1395.

Knopf, F., Hammond, C., Chekuru, A., Kurth, T., Hans, S., Weber, C. W., Mahatma, G., Fisher, S., Brand, M., Schulte-Merker, S., et al. (2011). Bone regenerates via dedifferentiation of osteoblasts in the zebrafish fin. *Dev. Cell* **20**, 713–724.

Lee, R. T. H., Asharani, P. V. and Carney, T. J. (2014). Basal keratinocytes contribute to all strata of the adult zebrafish epidermis. *PLoS One* **9,** e84858.

Mescher, A. L. (1976). Effects on adult newt limb regeneration of partial and complete skin flaps over the amputation surface. *J. Exp. Zool.* **195**, 117–128.

Metzger, D., Clifford, J., Chiba, H. and Chambon, P. (1995) Conditional site-specific recombination in mammalian cells using a ligand-dependent chimeric Cre recombinase. *Proc. Natl. Acad. Sci. U.S.A. 92*, 6991-6995.

Nakatani, Y., Nishidate, M., Fujita, M., Kawakami, A. and Kudo, A. (2008). Migration of mesenchymal cell fated to blastema is necessary for fish fin regeneration. *Dev. Growth Differ.* **50**, 71–83.

Nechiporuk, A. and Keating, M. T. (2002). A proliferation gradient between proximal and msxb-expressing distal blastema directs zebrafish fin regeneration. *Development* **129**, 2607–2617.

Poleo, G., Brown, C. W., Laforest, L. and Akimenko, M.-A. (2001). Cell proliferation and movement during early fin regeneration in zebrafish. *Dev. Dyn.* **221**, 380–390.

Rakers, S., Niklasson, L., Steinhagen, D., Kruse, C., Schauber, J., Sundell, K. and Paus, R. (2013). Antimicrobial peptides (AMPs) from fish epidermis: Perspectives for investigative dermatology. *J. Invest. Dermatol.* **133**, 1140–1149.

Sada, A., Jacob, F., Leung, E., Wang, S., White, B. S., Shalloway, D. and Tumbar, T. (2016). Defining the cellular lineage hierarchy in the interfollicular epidermis of adult skin. *Nat. Cell Biol.* **18**, 619–631.

Sandoval-Guzmán, T., Wang, H., Khattak, S., Schuez, M., Roensch, K., Nacu, E., Tazaki, A., Joven, A., Tanaka, E. M. and Simon, A. (2014). Fundamental differences in dedifferentiation and stem cell recruitment during skeletal muscle regeneration in two salamander species. *Cell Stem Cell* **14**, 174–187.

Shibata, E., Yokota, Y., Horita, N., Kudo, A., Abe, G., Kawakami, K. and Kawakami, A. (2016). Fgf signalling controls diverse aspects of fin regeneration. *Development* **143,** 2920-2929

Tassava, R. A. and Garling, D. J. (1979). Regenerative responses in larval axolotl limbs with skin grafts over the amputation surface. *J. Exp. Zool.* **208**, 97–110.

Thisse, C. and Thisse, B. (2008). High-resolution in situ hybridization to whole-mount zebrafish embryos. *Nat. Protoc.* **3**, 59-69.

Thornton, C. S. (1955). The effect of apical cap removal on limb regeneration in amblystoma larvae. *J Exp Zool.* **134**, 357-381.

Wada, H., Ghysen, A., Asakawa, K., Abe, G., Ishitani, T. and Kawakami, K. (2013). Wnt/Dkk negative feedback regulates sensory organ size in zebrafish. *Curr. Biol.* **23**, 1559–1565.

Wehner, D., Cizelsky, W., Vasudevaro, M., Özhan, G., Haase, C., Kagermeier-Schenk, B., Röder, A., Dorsky, R. I., Moro, E., Argenton, F., et al. (2014). Wnt/β-catenin signaling defines organizing centers that orchestrate growth and differentiation of the regenerating zebrafish caudal fin. *Cell Rep.* **6**, 467–481.

Yoshinari, N., Ishida, T., Kudo, A. and Kawakami, A. (2009). Gene expression and functional analysis of zebrafish larval fin fold regeneration. *Dev. Biol.* **325**, 71–81.

Yoshinari, N., Ando, K., Kudo, A., Kinoshita, M. and Kawakami, A. (2012). Colored medaka and zebrafish: Transgenics with ubiquitous and strong transgene expression driven by the medaka β-actin promoter. *Dev. Growth Differ.* **54**, 818–828.

Figures

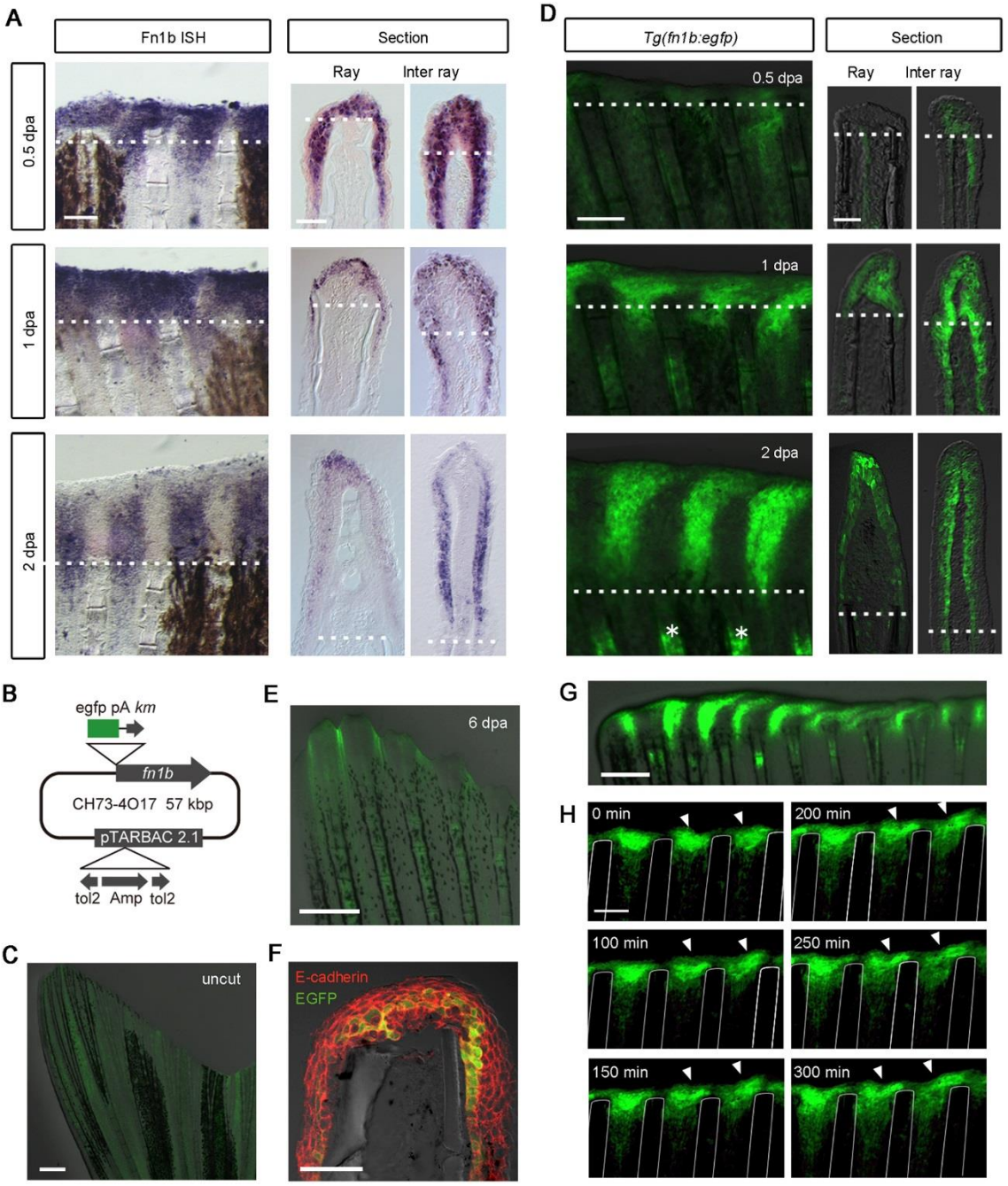

Fig. 1. Imaging of RE cells in *Tg(fn1b:egfp)* during fin regeneration.

(A) Whole mount ISH analysis of *fn1b* expression at 0.5, 1, and 2 dpa. Respective sections through the ray or inter-ray regions are shown on the right. *fn1b* was strongly induced in the RE by 1 dpa, and particularly in the inter-ray epithelium after 2 dpa. The dotted lines indicate the amputation plane. Scale bars, 100 μm (left) and 50 μm (right). (B) Map of the BAC construct used to generate the *Tg*

zebrafish. The *egfp* cassette was inserted by homologous recombination at the initiation site of the *fn1b* gene in the CH73-4O17 BAC. The tol2 cassette, which carries inverted orientations of the tol2 sequence and the intervening ampicillin resistance gene (amp), were introduced within the pTARBAC2.1 vector. pA, polyadenylation sequence; *km*, kanamycin resistance gene. (C) EGFP expression in the *Tg* fin before amputation. A very low level of EGFP fluorescence was observed throughout the uncut fin. Scale bar, 500 μm. (D) EGFP expression in the *Tg* fin after amputation. (left panels) and their respective sections. The respective sections through the ray or inter-ray regions are shown on the right. The dotted line indicates the amputation plane. Scale bars, 100 μm (left) and 50 μm (right). The asterisks show EGFP expression in the fin ray mesenchyme. (E) EGFP expression at 6 dpa. EGFP expression decreased after 2 dpa, and became weak at 6 dpa. Scale bar, 500 μm. (F) Immunohistochemical detection of E-cadherin (red) and EGFP (green) in a fin section of *Tg(fn1b:egfp)* at 1 dpa. Scale bar, 50 μm. (G) Whole mount image of the regenerating *Tg* fin at 2 dpa. Scale bars, 200 μm. It appears that $EGFP^+$ cells are recruited from the inter-ray regions and move laterally to cover the ray regions. For (A) and (C–G), n>5 fins or sections, respectively. (H) Time-lapse analysis of $EGFP^+$ cells in the *Tg(fn1b:egfp)*. Images were captured every 5 min from 24–29 hpa (n = 3 fins). Only the images at 0, 100, 150, 200, 250, and 300 min are shown. The arrowheads show representative $EGFP^+$ cells that may migrate from the inter-ray to the ray region. The white lines indicate the outlines of the fin rays. Scale bar, 100 μm.

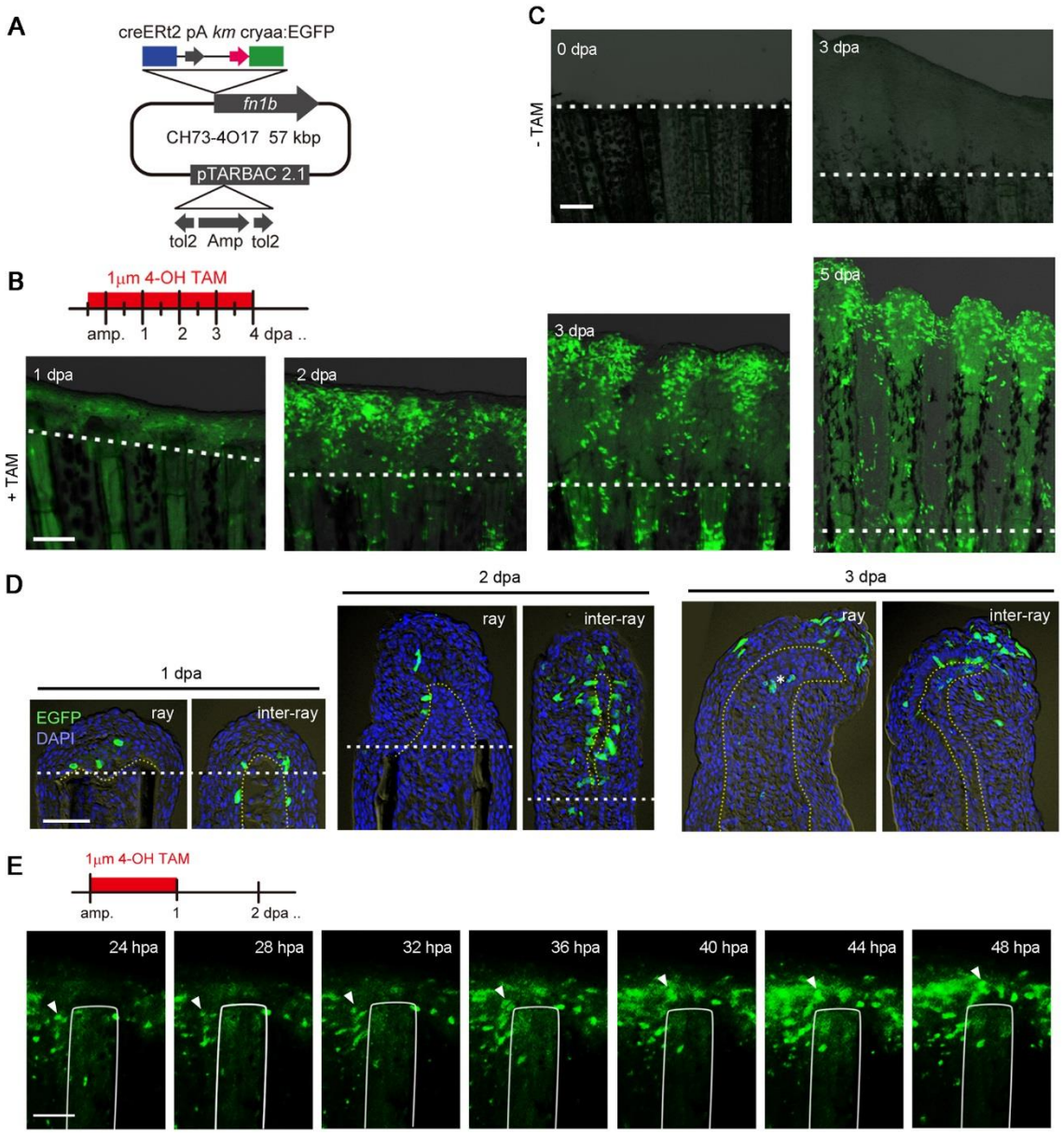

Fig. 2. Tracking cell fates of the RE using *Tg(fn1b:creERt2)*

(A) Map of the BAC construct used to generate the *Tg(fn1b:creERt2)*. The *creERt2* cassette was inserted in place of the *egfp* cassette at the site of the *fn1b* gene in the CH73-4O17 BAC. *cryaa*, *crystalline alpha a* promoter. (B) Labelling of *fn1b*-expressing cells by Cre-*loxP* recombination in the double *Tg(fn1b:creErt2; Olactb:loxP-dsred2-loxP-egfp)*. The *Tg* was treated with 1 μM 4-OH TAM from 12 hrs before amputation until 4 dpa. The dotted lines indicate the amputation planes. Scale bar, 200 μm. (C) Absence of $EGFP^{+}$ cells in the double *Tg* fin in the absence of 4-OH TAM treatment. Scale bar, 200 μm. (D) Longitudinal tissue sections of Cre-labelled fins at 1, 2, and 3 dpa, labelled as

in Fig. 2B. The dotted lines indicates the amputation planes. Scale bar, 50 μm. For (B–D), n>5 fins or sections, respectively. (E) Time-lapse analysis of Cre-labelled $EGFP^{+}$ cells from 24 hpa until 48 hpa. Images were captured every 1 hr (n = 3 fins). Only the images at 24, 28, 32, 36, 40, 44, and 48 hpa are shown. The arrowheads show a representative tracking of the same cell over time, indicating that the labelled cell indeed migrated from the inter-ray region to the ray region. The white lines show the outline of the fin ray bone. Scale bar, 100 μm.

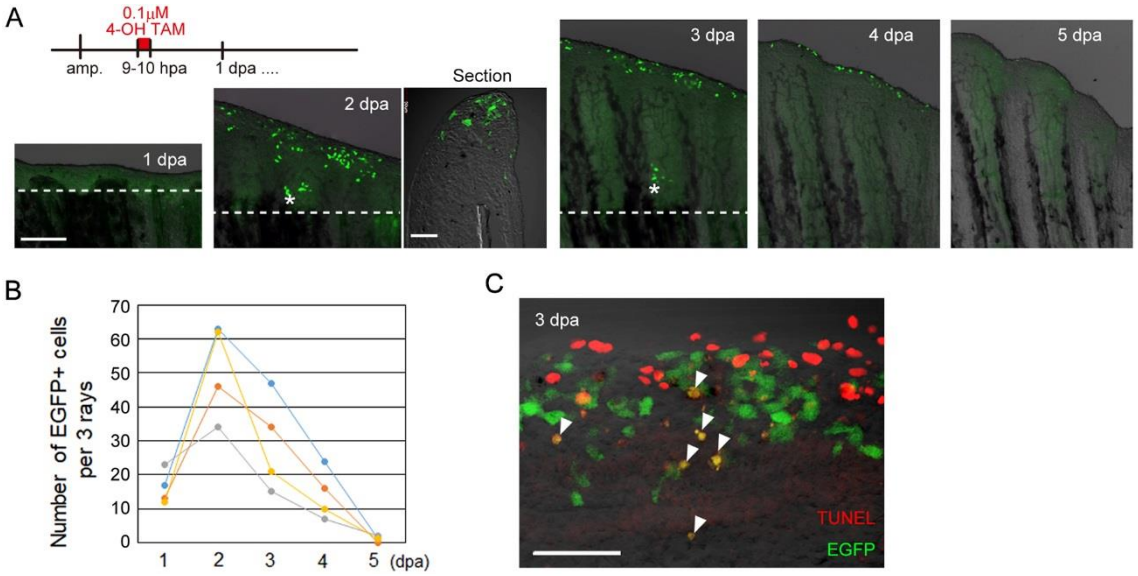

Fig. 3. Early RE cells are disposed of by apoptosis by 5 dpa during zebrafish fin regeneration

(A) Tracking of early RE cells that were pulse-labelled at 9–10 dpa with 0.1 μM 4-OH TAM. The labelled cells moved distally and disappeared by 5 dpa. Longitudinal section of the 2 dpa fin shows that the EGFP$^+$ cells localise to the tip of the wound epidermis. The dotted lines indicate the amputation planes. Scale bars, 200 μm and 50 μm, respectively. (B) Quantification of the number of EGFP$^+$ cells in (A). EGFP$^+$ cells in three adjacent rays were counted (n = 4 zebrafish). (C) Detection of the TUNEL$^+$ cells (red) and EGFP$^+$ cells derived from the early RE cells that were labelled by Cre-*loxP* recombination during 9-10 hpa. The arrowheads show the TUNEL$^+$ and EGFP$^+$ cells. Scale bar, 50 μm.

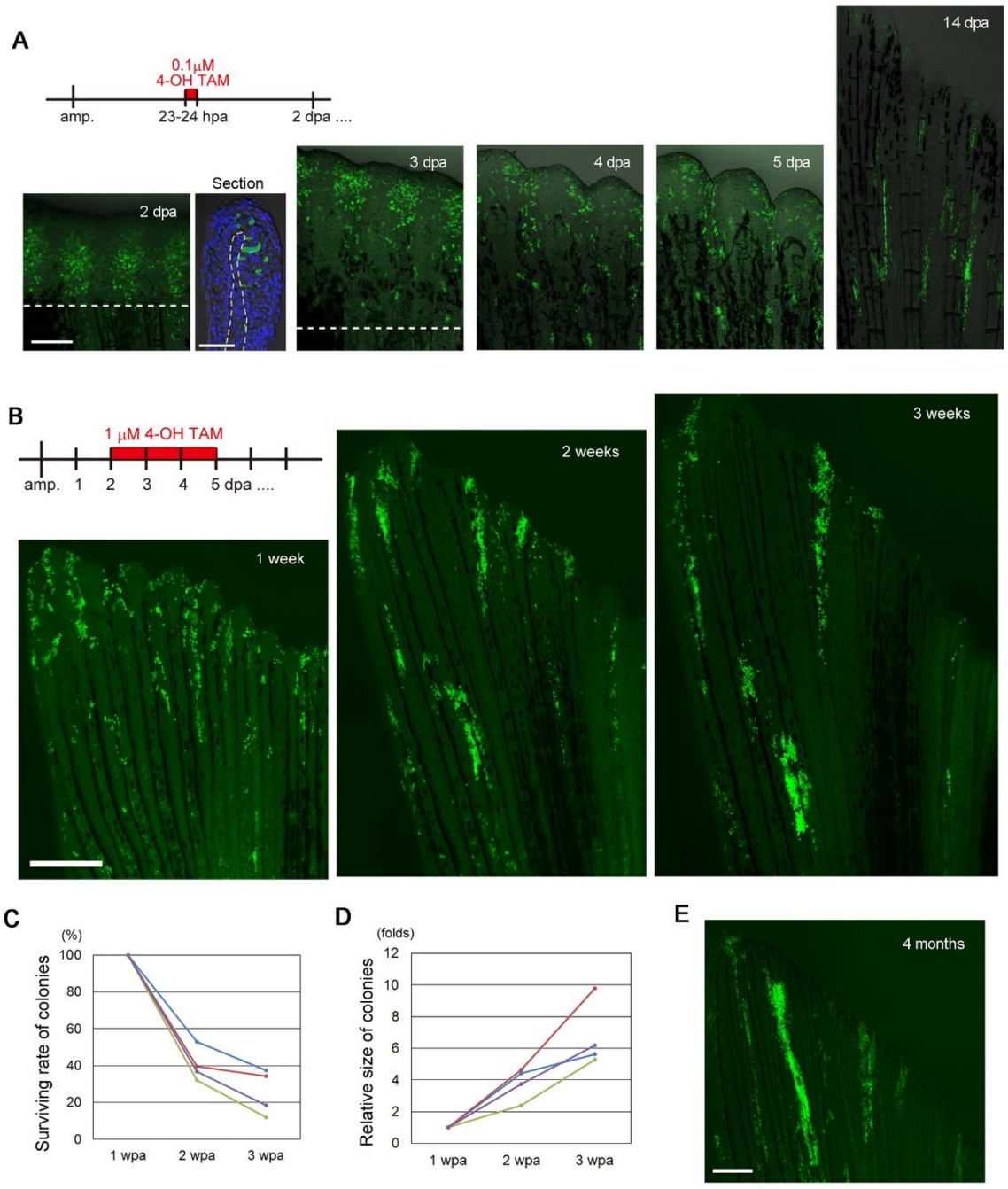

Fig. 4. Later emerging RE cells contribute to the regenerated epidermis

(A) Tracking of the progeny of *fn1b*-expressed RE cells that were labelled by Cre-*loxP* recombination during 23-24 hpa in the *Tg(fn1b*:creErt2;*Olactb:loxP-dsred2-loxP-egfp)*. Longitudinal section of the 2 dpa fin shows that $EGFP^{+}$ cells are found in both basal and non-basal cells in the RE. The dotted line indicates the amputation plane. Scale bars, 200 μm and 50 μm, respectively. (B) Tracking of the progeny of RE cells that were labelled by Cre-*loxP* recombination during 2-5 dpa. Cell colonies

derived from the Cre-labelled cells were evident at 1 wpa. However, whereas the size of the colonies grew over time, the number of colonies decreased. (C) Quantification of the number of colonies derived from the Cre-labelled cells in (B) at 1, 2, and 3 wpa (n = 4 zebrafish). Approximately 80% of the colonies disappeared between weeks 1 and 3. Bars denote the mean. (D) Quantification of the size of colonies derived from the Cre-labelled cells in (B) at 1, 2, and 3 wpa (n = 4 zebrafish). In contrast to the number of colonies, the colony size increased between 1 and 3 weeks. Bars denote the mean. (E) Tracking of the Cre-labelled RE-derived cells after four months. Progeny of the RE-derived cells were still retained in the epidermis, although their number was decreased relative to the number at 3 wpa. Scale bar, 500 μm.

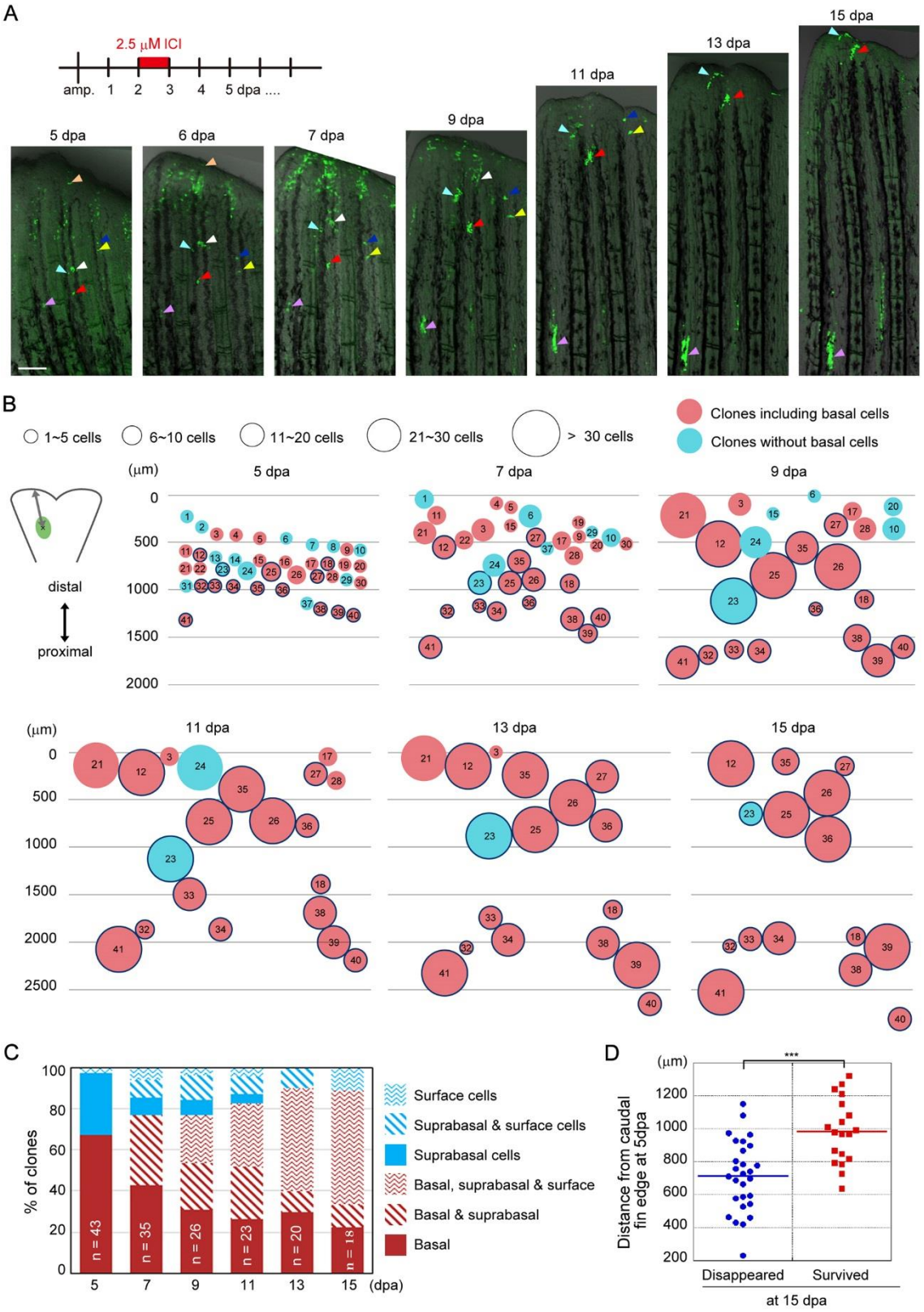

Fig. 5. Fate analysis of single *fn1b*-expressed RE cells

(A) Single clone tracking of the progeny of *fn1b*-expressed RE cells labelled by Cre-*loxP* recombination in the *Tg(fn1b:creErt2;Olactb:loxP-dsred2-loxP-egfp*. Labelling was performed using 2.5 μM ICI during 2–3 dpa. The coloured arrowheads indicate the respective positions of representative clones. Scale bar, 200 μm. The position of the purple arrowheads relative to the amputation site is approximately constant. It is noteworthy that clones of the Cre-labelled cells gradually moved in the caudal direction and disappeared at the fin edge. (B) Schematic illustration of the data from the single clone tracking analysis. Distances of clones from the caudal edge, sizes of the clones, and inclusion of basal cells are schematically expressed by the positions, sizes, and colours of the respective circles. n = 41 clones from 10 zebrafish. Many of the clones without basal cells and/or located in distal regions disappeared by 15 dpa. It is of note that an increase in cell number does not depend on the position of the clones, but rather occurs at random. The thick blue outline of the circles indicates the clones that survived beyond 15 dpa. (C) Ratios of individual epidermal clone types grouped by cell type composition. The ratios are expressed as percentage of cells among the surviving clones at each stage. At 5 dpa, most clones derived from the RE contained only basal or suprabasal cells. The suprabasal clones produced the surface cells and finally became the clones containing only surface cells at 15 dpa, whereas the basal clones produced the suprabasal and surface cells to become clones containing all three cell types. (D) Beeswarm plot of the respective positions of clones from the caudal fin tip at 5 dpa. The surviving clones at 15 dpa were originally located in the proximal regions at 5 dpa, whereas a significant number of distally-located clones at 5 dpa disappeared at 15 dpa (***p = 0.0000418). n = 19 (survived clones) and 29 (disappeared clones). Student's t-test (two-tailed) was performed to assess statistical significance. Bars denote the mean.

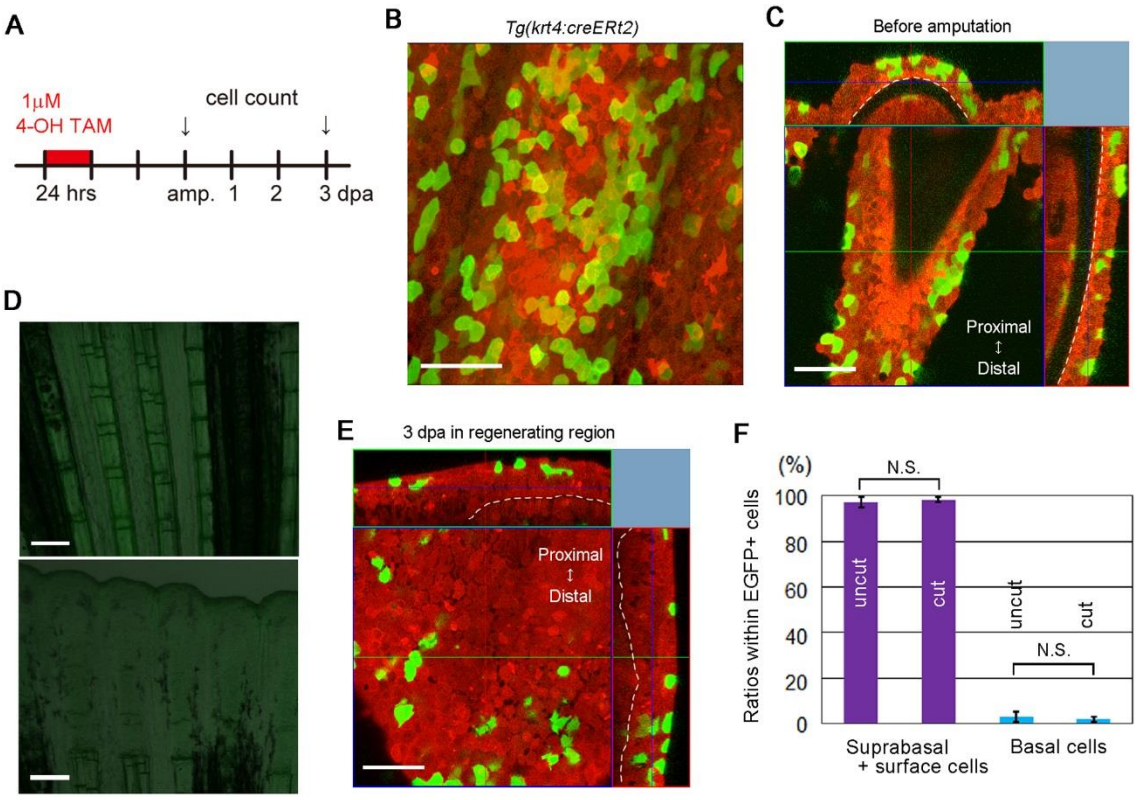

Fig. 6. Fate analysis of suprabasal and surface epidermal cells

(A) Experimental procedure used to conduct the fate analysis of surface and suprabasal cells. (B) A representative z-stack image of an uncut fin from a *Tg(krt4:creERt2; Olactb:loxP-dsred2-loxP-egfp*, in which the non-basal epidermal cells were labelled by treatment with TAM. Scale bar, 50 μm. A number of Cre-labelled cells are seen at two days after TAM treatment. (C) A confocal optical section of the *Tg* fin shown in Fig. 6B. The dotted lines indicate the basement membranes of the epidermis. The top and right images are tomographic images reconstituted from the z-stack data. The Cre-labelled cells are mostly seen in the suprabasal and surface cell layers. Scale bar, 50 μm. (D) Cre-mediated recombination without TAM treatment in an uncut fin (top) and a regenerating fin at 3 dpa (bottom) from *Tg(krt4:creERt2; Olactb:loxP-dsred2-loxP-egfp*). $EGFP^+$ cells were not observed (n = 3 for both groups). Scale bars, 200 μm. (E) A confocal optical section of a 3 dpa fin from *Tg(krt4:creERt2)* that were amputated 2 days after TAM treatment. The top and right images are tomographic images reconstituted from the z-stack data. The dotted lines indicate the basement membranes of the epidermis. The progeny of the Cre-labelled non-basal cells localised to the suprabasal and surface cell layers. Scale bar, 50 μm. (F) Quantification of the ratios of respective epidermal cell types within Cre-labelled $EGFP^+$ cells, before and after fin amputation. Although only a small fraction of labelled cells were seen in the basal epidermal layer, the ratio of basal cells within $EGFP^+$ cells did not change, comparing before and after amputation, suggesting that most of the suprabasal and/or surface cells maintained

their identities and did not de-differentiate into the basal cells during regeneration. Error bars denote mean± s.e.m.; Student's t-test (two-tailed) was performed to assess statistical significance (n = 27 images from 8 uncut fin and 28 images from 8 regenerating fin, respectively). N.S., not significant (p = 0.69).

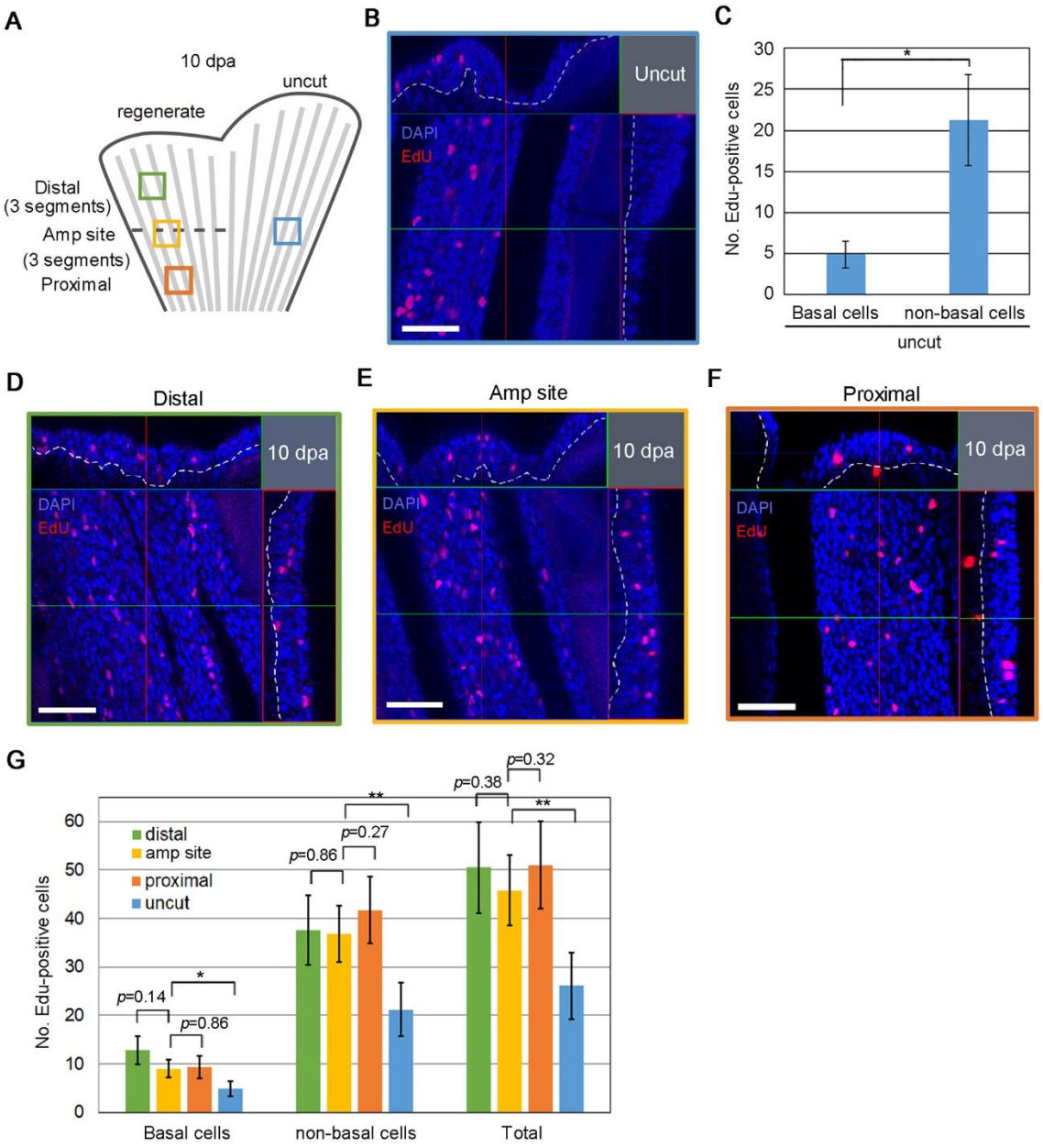

Fig. 7. Global cell proliferation replenishes epidermal cells

(A) Schematic diagram showing the process used for quantification of EdU$^+$ epidermal cells. The dorsal half of the fin was amputated at the middle of the central fin ray. The numbers of EdU$^+$ cells were scored in four fin areas of a 10 dpa fin (212 × 212 μm); the central region at the level of the amputation site (Amp site, yellow box), the distal region (three segments distal to the amputation site; Distal, green box), the proximal region (three segments proximal to the amputation site; Proximal, orange box), and the uncut region at the level of amputated site (blue box). Since the number of EdU$^+$ cells were nearly the same in the proximal and distal parts of the uncut fin region, scoring was done in the central region at the site of amputation. (B) Detection of EdU+ cells in the epidermis using

confocal optical sections in the uncut region (blue box in A). Confocal longitudinal and transverse optical sections are shown at the top and the right side, respectively. The vertical and horizontal red and green lines indicate the approximate sites of the optical sections. Nuclei were counterstained with 4′,6-diamidino-2-phenylindole (DAPI). The white dotted lines show the boundary of the epidermis and mesenchyme. Scale bar, 50 μm. (C) Quantification of the number of EdU^+ cells in B. The number of cells were counted on confocal images (n = 10 images from 5 zebrafish). Error bars denote mean± s.e.m.; Student's t-test (two-tailed) was performed to assess statistical significance. *$p < 0.05$.

(D-F) Detection of EdU+ cells in the epidermis using confocal optical sections in the distal region (D, green box in A), the central region (E, yellow box in A), and the proximal region (F, orange box in A). Nuclei were counterstained with DAPI. White dotted lines, the boundaries between epidermis and mesenchyme. Scale bars, 50 μm. (F) Quantification of the number of EdU^+ cells in D-F and comparison with those in uncut fin in C. The respective colours of the bars represent the regions shown in A. The number of cells were counted on confocal images (n = 10 images in different area of 5 zebrafish, respectively). Error bars denote mean± s.e.m.; Student's t-test (two-tailed) was performed to assess statistical significance. *$p < 0.05$; **$p < 0.005$.

Supplementary Information

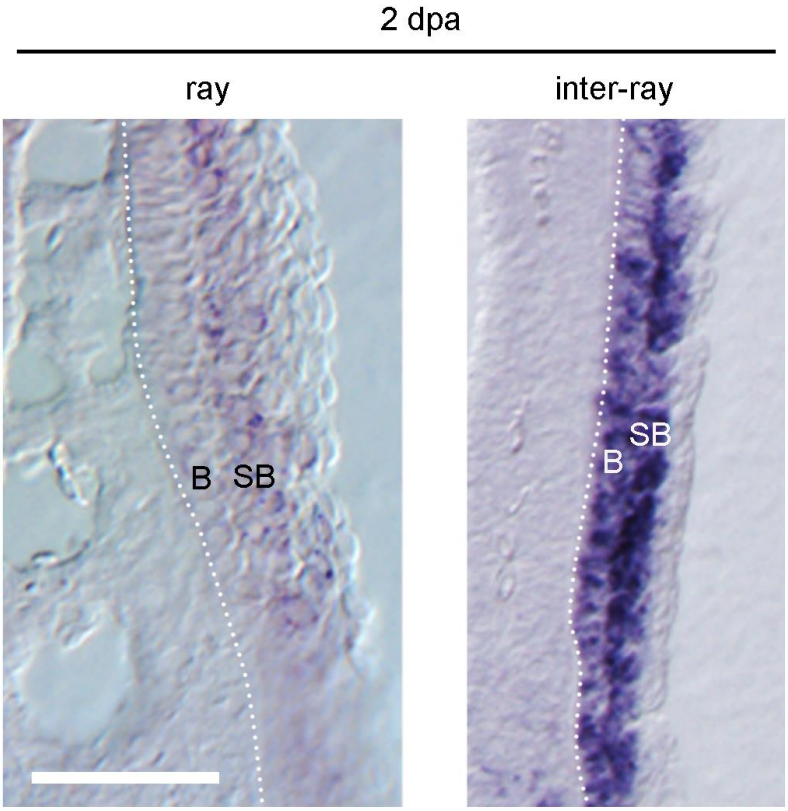

Fig. S1. *fn1b* expression in the ray and inter-ray regions of the RE.

The close-up view of *fn1b* expression at 2 days post amputation (dpa) in the ray and inter-ray regions, respectively. The expression is detected in the suprabasal cells (SB) of the RE and basal cells (B) of the inter-ray RE, but not of the ray region. The dotted lines indicate the boundaries between the epidermis and mesenchyme. Scale bar, 50 μm.

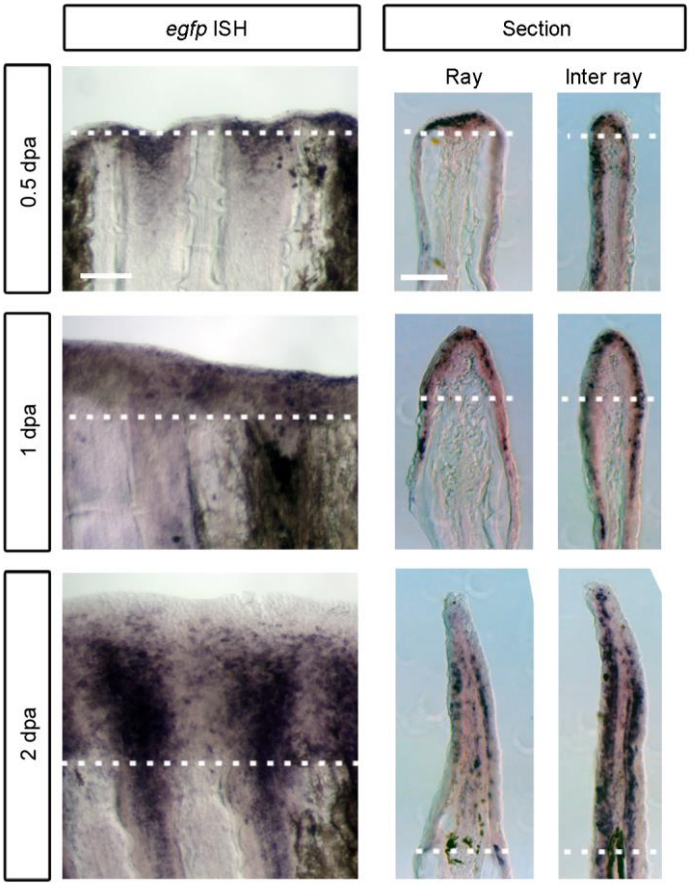

Fig. S2. *egfp* mRNA expression in the *Tg(fn1b:egfp)*.

Whole mount ISH analysis of the *egfp* expression in the *Tg(fn1b:egfp)* at 0.5, 1 and 2 dpa. Respective sections through the ray and inter-ray regions are shown on the respective right side. The dotted lines indicate the amputation plane. The expression is nearly the same with that of endogenous *fn1b* shown in Fig. 1A. Scale bars, 100 μm (whole-mounts) and 50 μm (sections).

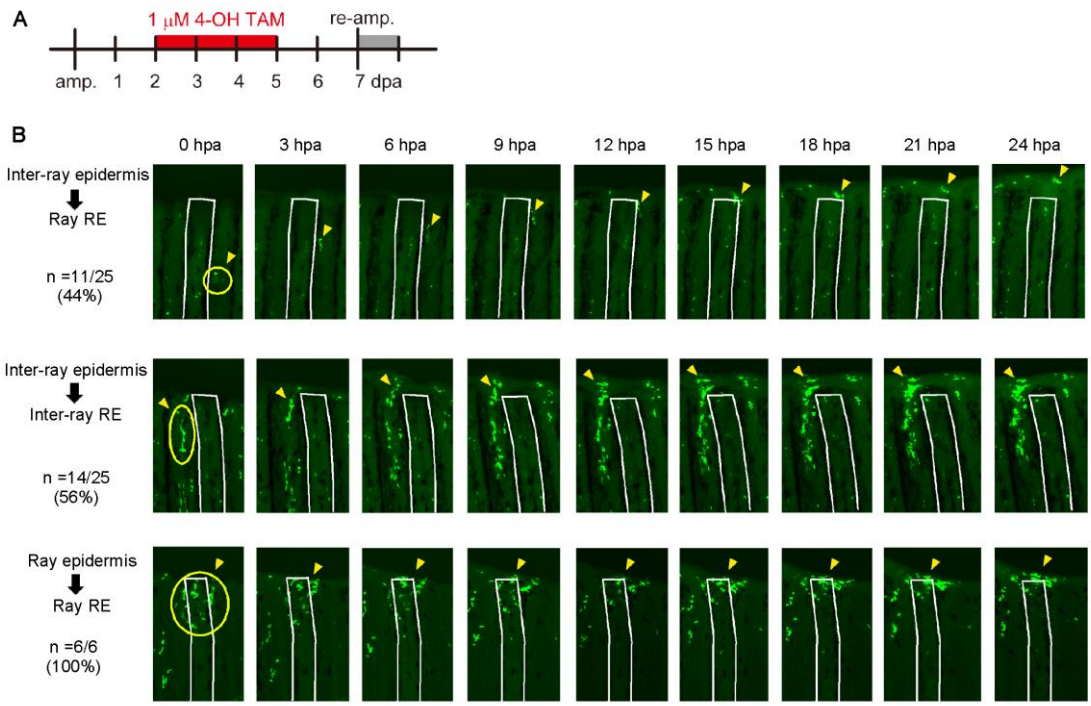

Fig. S3. Early process of the RE formation before 24 hpa.

(A) Experimental procedure for the fate analysis of epidermal cells that were pre-labelled by the Cre-*loxP* recombination in the *Tg(fn1b:creERt2;Olactb:loxP-dsred2-loxP-egfp)*. The *fn1b*$^{+}$ RE cells were labelled between 2 to 5 dpa. At 7 dpa, their fins were re-amputated and observed every 3 hrs until 24 hpa.

(B) Representative fates of pre-labelled epidermal cells that locate in the inter-ray region (top and middle) and the ray region (bottom), respectively. Clusters of EGFP^{+} cells were chosen and tracked their fates. The inter-ray epidermal cells either migrated to become the ray RE (top) or kept staying in the inter-ray region (middle). All of the ray epidermal cells did not migrate laterally, contributing to the ray RE.

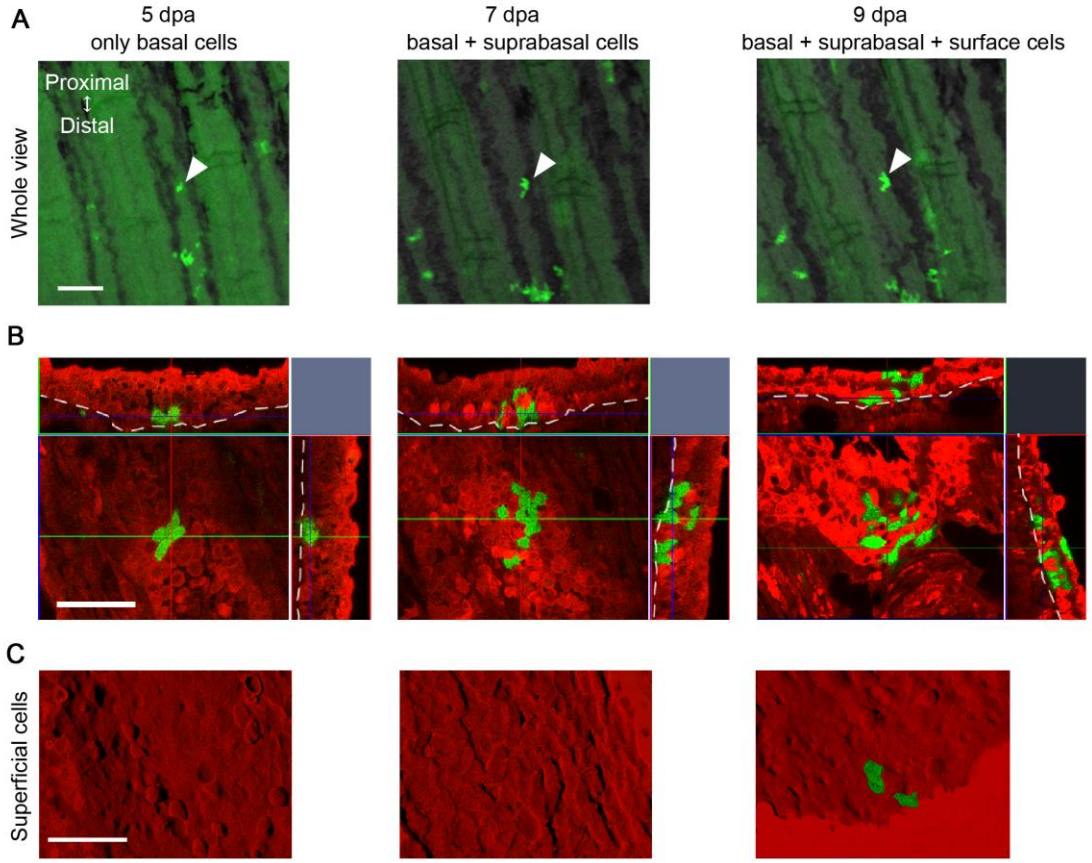

Fig. S4. Fate tracking of a single clone.

(A) Whole mount images of a representative clone (white arrowheads) at 5, 7, and 9 dpa. Scale bar, 100 μm.

(B) Confocal images of the same clone (No. 11) at respective stages. The top and right images are tomographic images reconstituted from the z-stack data. The dotted lines show the boundary between epidermal cells and mesenchymal cells. The clone contained only basal cells at 5 dpa, but produced suprabasal and surface cells at later stages. Scale bar, 50 μm.

(C) Confocal optical sections of the same clone (No. 11) focusing on the surface cells within the same region of the epidermis. Respective pictures show the same area and in the same direction with those in (B). Scale bar, 50 μm.

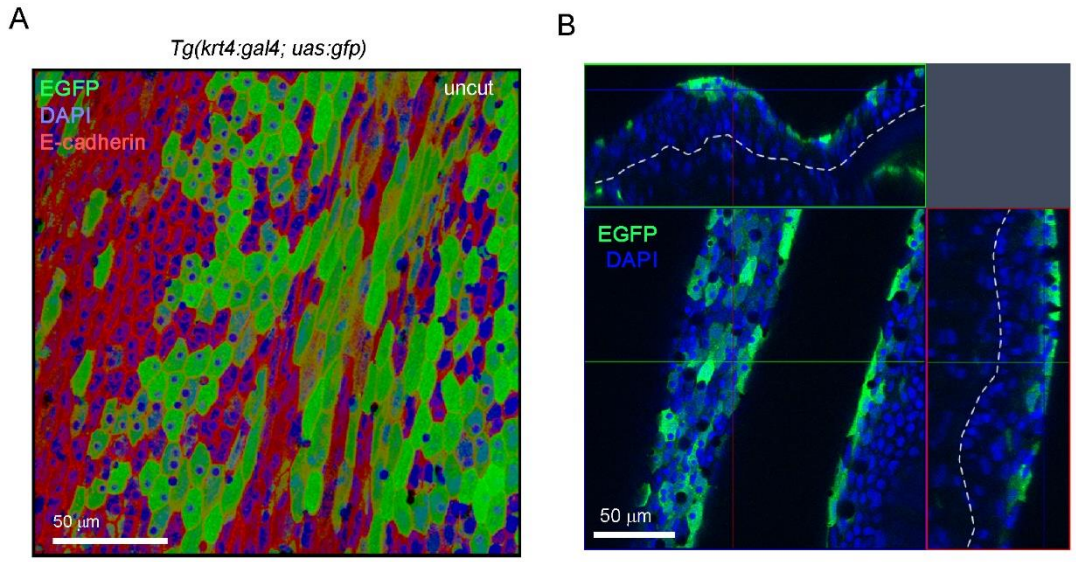

Fig. S5. Expression of EGFP in an uncut fin from a *Tg(krt4:gal4; uas:gfp)*.

(A) Immunohistochemical detection of E-cadherin (red) and EGFP (green) in an uncut fin from a *Tg(krt4:gal4; uas:gfp)*. The nuclei were counterstained with DAPI (blue). Scale bar, 50 μm.

(B) Confocal image of the *Tg(krt4:gal4; uas:gfp)* fin shown in (A). Top and right images are the tomographic images reconstituted from the z-stack data. The white dotted lines indicates the boundary between the epidermis and the mesenchyme. EGFP+ cells are mostly localised in the suprabasal and surface epidermal layers. Scale bar, 50 μm.

Table S1. Fates of respective clones derived from the RE.

Single clone tracking of the progeny of *fn1b*-expressed RE cells labelled by Cre-*loxP* recombination in the *Tg(fn1b:creErt2;Olactb:loxP-dsred2-loxP-egfp*. Labelling was performed using 2.5 μM ICI during 2–3 dpa, and the fates of respective clones were tracked until 15 dpa. Cell types and numbers composing the respective clones were determined every other day by analysing z-stack confocal images.

Click here to Download Table S1